Inelastic guiding of electrons in polymer nanocapillaries

S. Das,[1] B. S. Dassanayake,[1] M. Winkworth,[1] J. L. Baran,[1] N. Stolterfoht,[2] and J. A. Tanis[1]
[1]*Department of Physics, Western Michigan University, Kalamazoo, Michigan 49008, USA*
[2]*Hahn-Meitner-Institut Berlin GmbH, Glienickerstr. 100, D-14109 Berlin, Germany*
(Received 12 April 2007; published 31 October 2007)

Electron transmission through insulating polymer nanocapillary (diameter 200 nm and aspect ratio 50) foils has been investigated for incident energies 500 and 1000 eV. Significant intensities of transmitted electrons were observed for foil tilt angles up to ~10°, and corresponding observation angles with respect to the incident beam direction, a phenomenon referred to as *guiding*. The transmitted electron spectra show substantial energy losses that increase with the capillary tilt angle, in sharp contrast to previous results for slow positive ions and lower energy electrons. Despite apparent close encounters with the capillary walls, inelastically scattered electrons are found to be guided at angles coinciding with elastically scattered electrons. These results suggest a means to study the dynamics of electron interactions with insulating materials, which is complicated by charge buildup in conventional surface scattering studies.

DOI: 10.1103/PhysRevA.76.042716 PACS number(s): 34.50.Fa, 34.50.Dy, 34.80.Dp

The interaction of highly charged ions (HCI) with surfaces has been the subject of extensive research both experimentally and theoretically not only because of its potential application in the field of nanotechnology but also from the point of view of fundamental understanding [1,2]. In recent years, attention has centered on the transmission of HCI through nanocapillaries, with the reported *guiding* of slow positive ions (3 keV Ne^{7+}) through insulating nanocapillary foils of polyethylene terephthalate (PET) by Stolterfoht *et al.* [3]. Surprisingly, ion transmission with negligible charge change was observed for foil tilt angles up to $\psi=20°$ with respect to the incident beam direction, indicating distant encounters with the capillary walls. It was proposed that this result was due to a self-organizing charge up of the inner walls of the capillaries [3] that, after a characteristic charging time, deflects the traversing ions causing them to be "guided" through the sample along the capillary axis. In subsequent work by these authors additional properties of slow ion guiding in PET foils were investigated [4,5].

Experimental and theoretical works by other investigators have been conducted for slow (~1–10 keV) positive ions [6–11], and in one instance fast 200 MeV Ti^{12+} ions [12] were used to determine the alignment of nanocapillaries in a sample. Notably, for slow H_2 molecular ions [13] negligible fragmentation occurred as a result of passage through the nanocapillary foils, indicating the strength of the guiding effect. In addition to polymer foils, ion guiding has been studied for nanocapillary samples of SiO_2 [7], alumina [10,12], and tapered glass [11]. In all cases, the surfaces of the insulating nanocapillary samples were coated with a thin conducting layer, e.g., gold or aluminum, to prevent charging of the sample during the measurements. Just recently, guiding for lower energy 200–350 eV electrons in Al_2O_3 nanocapillary foils has been reported [14].

In this Communication we report the guiding of fast electrons through insulating PET nanocapillaries. The measurements focus on the dependence of the transmitted electron intensity on the nanocapillary tilt angle ψ and on the corresponding electron energy spectra. The angular distributions of the transmitted electrons demonstrate that electrons are guided through the capillaries, but with intensities that are strongly attenuated compared to positive ions [3–13]. Significantly, the transmitted electrons undergo considerable energy losses that dominate the energy spectra with the fractional loss increasing with capillary tilt angle, a result not observed for slow positive ions or for lower energy electrons [14]. Despite losing energy, presumably due to close encounters with the capillary walls, these inelastically scattered electrons show clear evidence of guiding. The results suggest that inelastic electron guiding might be used to study the dynamics of electrons interacting with insulators, which, in the case of conventional surface scattering, is complicated by charge buildup on the insulator surface.

The present measurements were performed at Western Michigan University. PET foil capillaries of 200 nm diameter and 10 μm length (aspect ratio=50) were prepared at the Hahn-Meitner-Institute, Berlin by etching ion tracks created by high-energy projectiles in a solid [3]. The foil was mounted in a two-dimensional goniometer that allowed precise positioning (tilt angle rotation about a vertical axis and azimuthal rotation about a horizontal axis) with respect to the incident beam. The electrons were obtained from a simple filament source and collimated to diameter of 1.5 mm. Transmitted electrons were analyzed with a parallel-plate analyzer located a few centimeters behind the sample and counted with a channeltron multiplier (CEM). The background pressure in the scattering chamber was less than 10^{-6} Torr.

The "zero position" for maximum transmission of electrons directly through the sample along the capillary axis was located by varying the goniometer tilt ψ and azimuthal angles in small steps, and by varying the observation angle θ of the electron spectrometer. The inset to Fig. 1 shows the tilt ψ and observation θ angles, both measured with respect to the incident beam direction. When this position was located (defined as $\psi=0°$), the observation angle was fixed (at $\theta=0°$) and the tilt angle varied in small steps to determine the profile for direct transmission of electrons through the foil, for which a FWHM $\Gamma_{direct}=0.65°$ was found. This width is a convolution of the half-widths due to the aspect ratio ($\Gamma_{aspect}=0.57°$), the beam collimation ($\Gamma_{coll}\sim 0.25°$), and the degree of parallelism (Γ_{par}) of the capillaries inside the

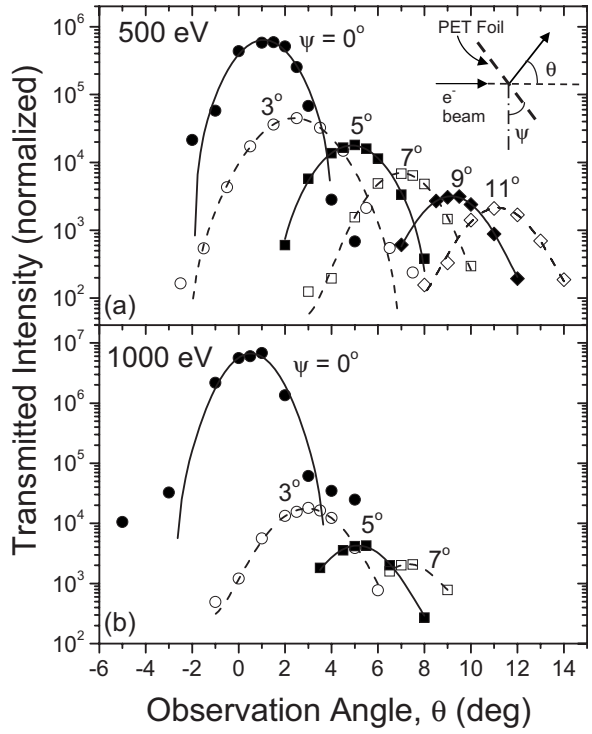

FIG. 1. Angular distributions of the integrated normalized transmitted electron intensities plotted as a function of observation angle θ for the indicated tilt angles ψ for (a) 500 eV and (b) 1000 eV incident electrons. The inset shows a schematic of these angles with respect to the incident beam.

sample. Combining these widths in quadrature gives a value $\Gamma_{par} \sim 0.2°$ for the parallelism of the capillaries inside the foil, indicating a high degree of alignment.

To investigate guiding phenomena, the sample was tilted with respect to the straight-through position and the observation angle changed accordingly. A significant intensity of transmitted electrons was found for tilted sample angles, and correspondingly shifted observation angles, as shown in Fig. 1 for incident 500 and 1000 eV electrons. The transmitted intensities were normalized to incident beam currents of ~0.3 and ~0.8 nA measured on the sample for 500 and 1000 eV, respectively, and were determined under equilibrium conditions, i.e., after a sufficient time that charge-up effects on the inner walls of the nanocapillaries had reached steady-state conditions (see Ref. [3]). For the present work, the electron beam was typically started 2–3 hours prior to beginning the measurements.

Clear evidence for electron guiding is seen in Fig. 1, up to tilt angles of $\psi = 11°$ for 500 eV and up to $\psi = 7°$ for 1000 eV. A plot of the centroid observation angle vs the tilt angle (not shown) reveals that θ depends linearly on ψ as expected (note that θ may not be exactly equal to ψ in Fig. 1 because of mechanical offsets in the measured angles). The guided intensities are seen to decrease exponentially (note the logarithmic scale), as observed for slow positive ions in PET samples [3–5]. The angular widths of the guided electron distributions shown in Fig. 1 do not change noticeably with tilt angle, but no particular significance should be attached to this result due to a spectrometer angular resolution of about 2.3°, as measured for electrons from the bare filament. In future studies a spectrometer with higher resolution will be utilized.

Figures 2 and 3 show the measured electron energy spectra obtained for the centroid observation angles ($\theta \simeq \psi$) for 500 and 1000 eV incident electrons, respectively. Not only does the overall intensity decrease strongly as the tilt angle increases, the spectra also show significant energy losses for the transmitted electrons. In fact, these *inelastic* contributions dominate the spectra with the fractional loss increasing and extending to lower values of electron energy as ψ increases. This energy loss is quite unexpected in view of earlier results for slow positive ions [3–11], and the recent results for 200–350 eV electrons in Al_2O_3 [14], for which no appreciable loss was observed even for rather large tilt angles.

To quantify the energy losses, we have evaluated separately the elastic and inelastic contributions to the transmitted electron intensity. To determine the separate contributions, it is observed that the electron energy spectrum for ψ

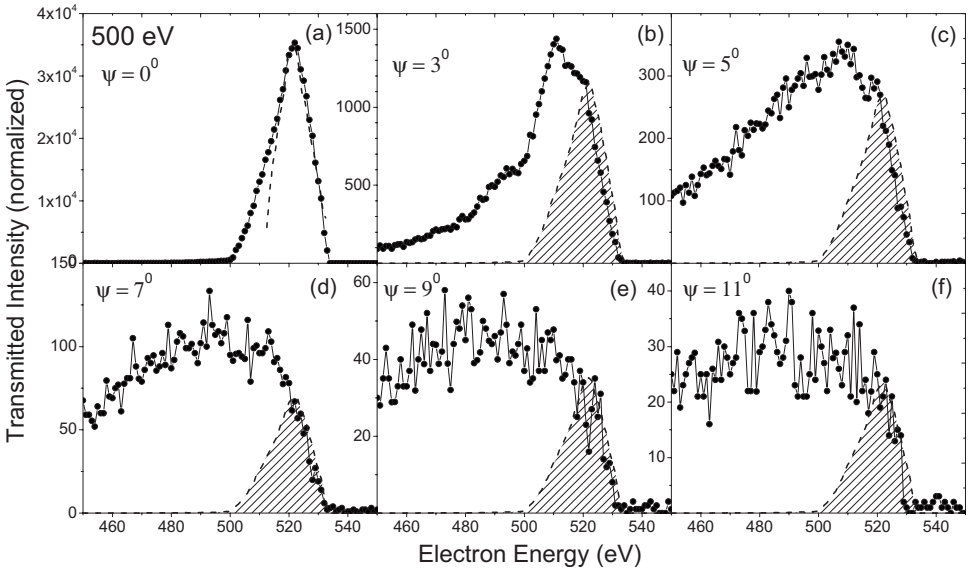

FIG. 2. Measured electron energy spectra for angles $\theta \simeq \psi$ showing the increasing fractional electron energy loss vs ψ for incident 500 eV electrons. The dashed curve in (a) shows the energy spectrum obtained for electron emission from the bare filament normalized to the spectrum for $\psi = 0°$. The shaded areas in (b)–(f) show the spectrum for $\psi = 0°$ normalized to the spectra for $\psi > 0°$, indicating the elastic contribution to the individual spectra.

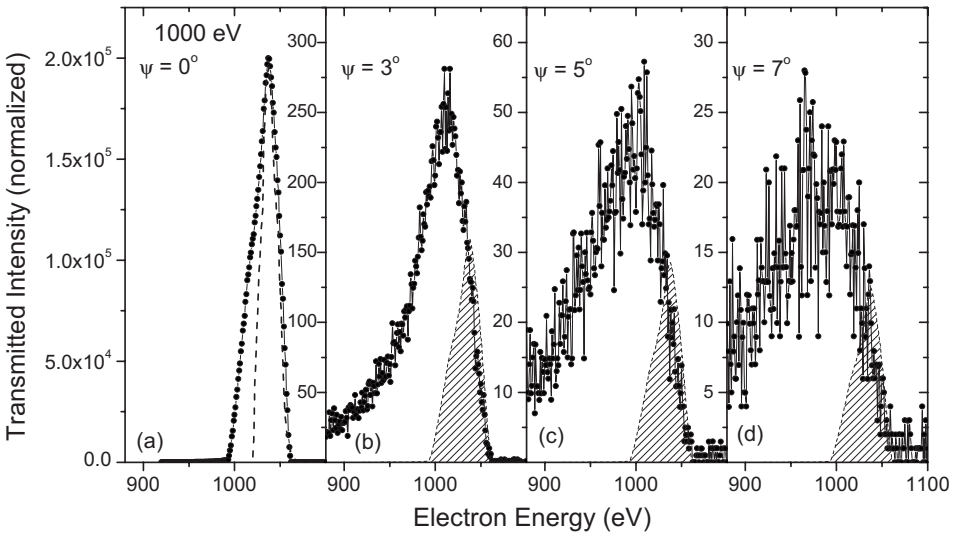

FIG. 3. Measured electron energy spectra for angles $\theta \simeq \psi$ showing the increasing fractional electron energy loss vs ψ for incident 1000 eV electrons. See caption for Fig. 2.

$=0°$ has nearly the same profile and width as the spectrum measured for the electron beam obtained from the bare filament as shown by the dashed curves in Figs. 2(a) and 3(a). [The small inelastic contribution on the low-energy side of each $\psi=0°$ peak can be attributed to the angular spread of the incident beam and to the capillary nonparallelism, which had full width at half maximum (FWHM) values of $\sim 0.25°$ and $\sim 0.2°$, respectively, as noted above]. This result indicates that for $\psi=0°$, electrons are transmitted through the foil with negligible interactions with the capillary walls, and consequently, any deviation from the measured $\psi=0°$ energy profile for tilt angles $\psi>0°$ is significant. The deviation can be determined by superimposing the spectrum for $\psi=0°$ on the corresponding spectra for $\psi>0°$ and normalizing to the intensities of these latter spectra. When this is done, it is found that the high energy cutoff of the spectra for $\psi>0°$ matches that for $\psi=0°$, as seen in Figs. 2(b)–2(f) and in Figs. 3(b)–3(d), showing the existence of an elastic contribution for all tilt angles. In this way the elastic contribution is determined directly and the inelastic contribution is obtained by subtraction.

Following the same procedure for the angular spectra collected for each given tilt angle ψ the angular transmission profiles can be separately determined for the elastic and inelastic contributions, as shown in Fig. 4 for 500 eV electrons. Significantly, the elastic and inelastic angular centroids coincide and are equal to the tilt angle, i.e., $\theta \simeq \psi$, showing convincingly that the inelastically scattered electrons are guided.

Having determined the angular profiles for the elastic and inelastic contributions, the exponential decay rates can be determined directly from the centroid spectra for $\psi>0°$, i.e., $\theta \simeq \psi$, giving the results shown in Figs. 5(a) and 5(b). To represent the integrated measured intensity for all tilt angles including $\psi=0$, a *direct* contribution corresponding to the large transmitted electron intensity at $\psi=0°$ must be included. From geometrical considerations, it can be shown that this contribution, which is due to the convolution of the capillary aspect ratio, the beam collimation, and capillary nonparallelism as discussed above, decreases nearly linearly for $\psi>0°$. From the measured value of $\Gamma_{direct}=0.65°$ (see above) for $\psi=\theta=0°$, the direct contribution can be calculated as indicated by the curves in Figs. 5(a) and 5(b). This contribution decreases very rapidly as expected.

The decay rates for the elastic and inelastic contributions for transmitted electrons are listed in Table I and compared with the results obtained by Hellhammer *et al.* [15,16] for positive ions. In that work, the *characteristic guiding angle* ψ_c was defined as the tilt angle for which the transmitted intensity falls to $1/e$. These authors found that $\sin^{-2}\psi_c$ for slow positive ions is a universal and linear function of the

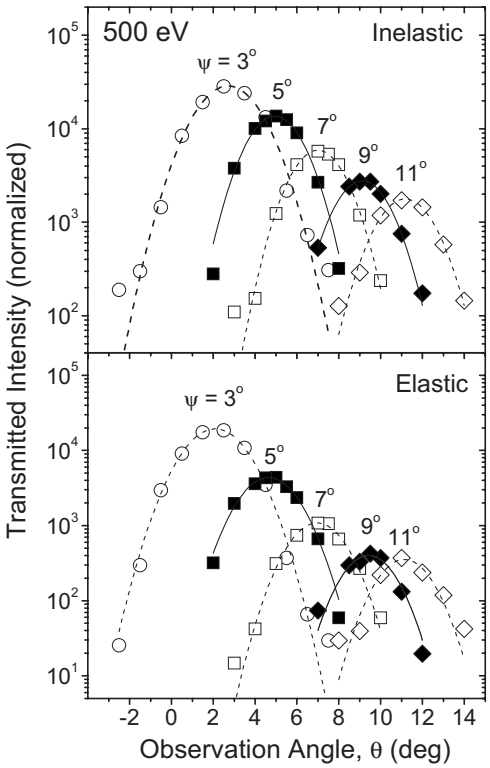

FIG. 4. Angular transmission profiles for the inelastic and elastic contributions to the measured electron energy spectra for each tilt angle investigated for 500 eV electrons. Note that the elastic and inelastic centroids coincide and are equal to the tilt angle, i.e., $\theta \simeq \psi$, indicating that inelastically scattered electrons are guided (see text).

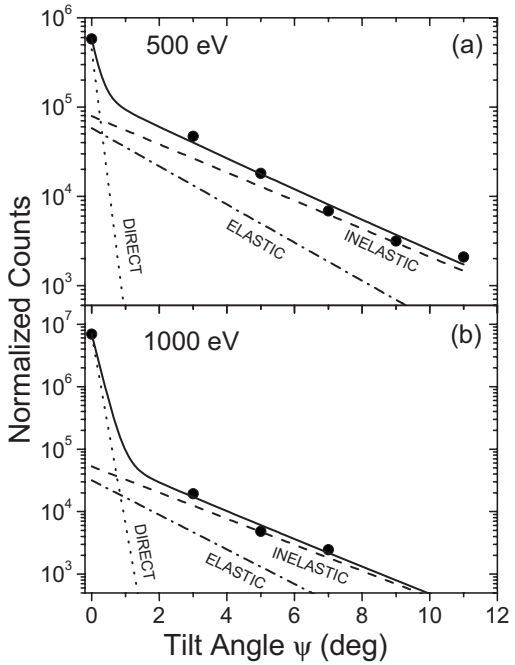

FIG. 5. Relative transmission intensities vs tilt angle for incident 500 and 1000 eV electrons. The elastic and inelastic decay curves were determined by fitting an exponential function to their respective contributions obtained from the data of Figs. 2 and 3. In addition, the direct contribution represents the large measured transmission fraction near $\psi=0°$ corresponding to electrons passing through the capillaries without interacting with the capillary walls (see text).

incident particle energy divided by its charge, i.e., E/q [15,16]. It is seen that the values of ψ_c obtained in the present work for electrons are smaller (representing a faster decay) than the corresponding values for ions, and, furthermore, the values of ψ_c are quite different for the elastic and inelastic contributions. It remains for future work to determine if a universal function exists for electron guiding, and how this function may differ for the elastic and inelastic contributions.

The present analysis indicates that three contributions—direct, elastic, and inelastic—are needed to represent the transmitted electron intensity. Although the inelastic contribution dominates the spectra for $\psi>0°$, there remains an elastic contribution for all tilt angles for which electron transmission was measured. As noted, the inelastically transmitted electrons are clearly guided as demonstrated by the data of Fig. 4. The large inelastic contribution suggests that insufficient (negative) charge is deposited on the inner walls of the capillaries to electrostatically prevent the traversing electrons from interacting strongly with the walls. As a consequence, some electrons are lost in the capillaries and those that make it through lose energy. Although inelastic interactions would be expected to lead to excitation and ionization of the capillary surfaces, the dynamics of inelastic electron guiding are not well understood.

TABLE I. Values of the characteristic guiding angles ψ_c for the elastic and inelastic contributions to the measured electron energy spectra in the present work for electron transmission through PET nanocapillaries compared with the values determined for slow positive ions, also for PET foils.

	ψ_c (degrees)		
E/q (eV)	Elastic	Inelastic	Ions
500	2.0	2.8	4.7[a]
1000	1.6	2.1	2.9[a]

[a]From References [15,16].

Previously, inelastic scattering was observed by Nebiki *et al.* [17] for incident 2 MeV He^+ ions traversing tapered SiO_2 capillaries at a tilt angle of 0°, but the inelastically transmitted ions were attributed to penetration of the capillary walls and not to guiding. In fact, no inelastic guiding was reported in that work. Moreover, the charge state of the transmitted ions was not measured, so it is not known if charge changing occurs or not, in contrast to the present work for incident electrons in which no charge change obviously takes place. Additionally, for a capillary tilt angle of just 2°, these authors reported negligible elastic transmission, but substantial inelastic transmission, of unknown emerging charge state, attributed to reflection from the capillary wall or to penetration through the wall. In contrast, we observe elastic transmission for all tilt angles for which guiding was observed.

The phenomenon of electron transmission and guiding through nanocapillaries, and particularly investigation of the associated inelastic processes, could provide a means to study fundamental interactions between electrons and insulators, which, unlike charged particle interactions with metals [18], have not been extensively studied by conventional surface scattering due to charge buildup on the insulator surface. Thus, studies with insulating nanocapillaries could lead to insight, concerning the production and guiding of secondary electrons [19], the excitation or ionization of core electrons giving rise to Auger processes, and the degradation of insulating polymers when irradiated by charged particles [20]. Moreover, the relatively weak C-C bonds in PET are easily broken by electron bombardment, causing physical or chemical degradation as a result of inelastic processes. Electron guiding through nanocapillaries might also be used to produce nanometer sized beams in electron microscopes, or to create pixel sizes smaller than those currently possible to enable higher resolution information displays.

In summary, we have demonstrated that electron transmission through insulating PET nanocapillary foils is dominated by an inelastic contribution that increases with the foil tilt angle. Despite significant energy losses, it is convincingly demonstrated that inelastically scattered electrons are still guided through the capillaries, a result that sharply contrasts with previous results for positive ions and for electrons. It is suggested that these inelastic processes are due to insufficient charge deposition on the inner walls of the capillaries, thereby permitting close encounters of traversing electrons with the capillary walls. Consequently, inelastic electron guiding may provide a means to study the dynamics of electron interactions with insulators.

We acknowledge assistance from David Cassidy in making the measurements.

[1] A. Arnau, F. Aumayr, P. M. Echenique, M. Grether, W. Heiland, J. Limburg, R. Morgenstern, P.Roncin, S. Schippers, R. Schuch, N. Stolterfoht, P. Varga, T. J. M. Zouros, H. P. Winter, Surf. Sci. Rep. **27**, 113 (1997), and references therein.
[2] Y. Yamazaki, Phys. Scr., T **73**, 293 (1997).
[3] N. Stolterfoht, J.-H. Bremer, V. Hoffmann, R. Hellhammer, D. Fink, A. Petrov, and B. Sulik, Phys. Rev. Lett. **88**, 133201 (2002).
[4] N. Stolterfoht, V. Hoffmann, R. Hellhammer, Z. D. Pešić, D. Fink, A. Petrov, and B. Sulik, Nucl. Instrum. Methods Phys. Res. B **203**, 246 (2003); N. Stolterfoht, R. Hellhammer, Z. D. Pešić, V. Hoffmann, J. Bundesmann, A. Petrov, D. Fink, B. Sulik, M. Shah, K. Dunn, J. Pedregosa, and R. W. Mc Cullough, *ibid.* **225**, 169 (2004); N. Stolterfoht, R. Hellhammer, Z. D. Pešić, V. Hoffmann, J. Bundesmann, A. Petrov, D. Fink, and B. Sulik, Vacuum **73**, 31 (2004); Surf. Coat. Technol. **196**, 389 (2005).
[5] R. Hellhammer, P. Sobochinski, Z. D. Pešić, J. Bundesmann, D. Fink, and N. Stolterfoht, Nucl. Instrum. Methods Phys. Res. B **232**, 235 (2005); R. Hellhammer, Z. D. Pešić, P. Sobochinski, D. Fink, J. Bundesmann, and N. Stolterfoht, *ibid.* **233**, 213 (2005).
[6] Gy. Vikor, R. T. Rajendra Kumar, Z. D. Pešić, N. Stolterfoht, and R. Schuch, Nucl. Instrum. Methods Phys. Res. B **233**, 218 (2005).
[7] M. B. Sahana, P. Skog, Gy. Vikor, R. T. Rajendra Kumar, and R. Schuch, Phys. Rev. A **73**, 040901(R) (2006).
[8] K. Schiessl, W. Palfinger, K. Tókési, H. Nowotny, C. Lemell, and J. Burgdörfer, Phys. Rev. A **72**, 062902 (2005).
[9] N. Stolterfoht, R. Hellhammer, J. Bundesmann, D. Fink, Y. Kanai, M. Hoshino, T. Kambara, T. Ikeda, and Y. Yamazaki, Phys. Rev. A **76**, 022712 (2007).
[10] S. Mátéfi-Tempfli, M. Mátéfi-Tempfli, L. Piraux, Z. Juhász, S. Biri, É. Fekete, I. Iván, F. Gáll, B. Sulik, G. Víkor, J. Pálinkás, and N. Stolterfoht, Nanotechnology **17**, 3915 (2006).
[11] T. Ikeda, T. M. Kojima, Y. Iwai, Y. Kanai, T. Kambara, T. Nebiki, T. Narusawa, and Y. Yamazaki, J. Phys.: Conf. Ser. **58**, 68 (2007).
[12] H. F. Krause, C. R. Vane, F. W. Meyer, and H. M. Christen, J. Phys.: Conf. Ser. **58**, 323 (2007).
[13] N. Stolterfoht, R. Hellhammer, P. Sobocinski, Z. D. Pešić, J. Bundesmann, B. Sulik, M. B. Shah, K. Dunn, J. Pedregosa, and R. W. McCullough, Nucl. Instrum. Methods Phys. Res. B **235**, 460 (2005).
[14] A. R. Milosavljević, Gy. Víkor, Z. D. Pešić, P. Kolarž, D. Šević, B. P. Marinković, S. Mátéfi-Tempfli, M. Mátéfi-Tempfli, and L. Piraux, Phys. Rev. A **75**, 030901(R) (2007).
[15] R. Hellhammer, Ph.D. thesis, Hahn-Meitner-Institute, Berlin, 2006 (unpublished).
[16] R. Hellhammer, J. Bundesmann, D. Fink, and N. Stolterfoht, Nucl. Instrum. Methods Phys. Res. B **258**, 159 (2007).
[17] T. Nebiki, T. Yamamoto, T. Narusawa, M. B. H. Breese, E. J. Teo, and F. Watt, J. Vac. Sci. Technol. A **21**, 1671 (2003).
[18] M. Rösler, Appl. Phys. A **61**, 595 (1995).
[19] Z. G. Song, C. K. Ong, and H. Gong, Appl. Surf. Sci. **119**, 169 (1997).
[20] A. Macková, V. Havránek, V. Švorčík, N. Djourelov, and T. Suzuki, Nucl. Instrum. Methods Phys. Res. B **240**, 245 (2005).